

## SEISMOTECTONICS OF THE CALABRIAN ARC \*

C. GASPARINI<sup>1</sup>, G. IANNACONE<sup>2</sup>, P. SCANDONE<sup>3</sup> and R. SCARPA<sup>2</sup>

<sup>1</sup> *Istituto Nazionale di Geofisica, Rome (Italy)*

<sup>2</sup> *Osservatorio Vesuviano, Ercolano, Naples (Italy)*

<sup>3</sup> *Istituto di Geologia, Pisa (Italy)*

(Received June 3, 1981; revised version accepted October 7, 1981)

### ABSTRACT

Gasparini, C., Iannaccone, G., Scandone, P. and Scarpa, R., 1982. Seismotectonics of the Calabrian arc. *Tectonophysics*, 84: 267–286.

Relocation of intermediate and deep earthquakes of Tyrrhenian Sea area through joint hypocenter determination for the period 1962–1979, has allowed a more detailed definition of the geometry of this peculiar Benioff zone. Earthquakes dip along a quasi-vertical plane to 250 km depth; there is a 50° dip in the 250–340 km depth range, and a low dip angle to 480 km depth. The structure sketched from the hypocenters is almost continuous, but most energy has been released in the 230–340 km depth interval. An evaluation of fault plane solutions of intermediate earthquakes in this area indicates predominance of down-dip compressions in the central part of the slab. At the border, strike-slip motion occurs independent of depth. Some earthquakes that occurred at intermediate depth (less than 100 km) along the Ionian margin of Calabria show predominance of reverse faulting, with the P-axis oriented SE–NW. However, shallow earthquakes in the Calabria–Sicily region indicate a more complex motion, with predominance of normal faulting. A possible interpretation of these features according to the available geological history, which involves subduction of continental lithosphere, is discussed.

### INTRODUCTION

The Calabrian arc is the region of Italy that is characterized by the most intense geodynamic activity, as can be deduced from the historical seismic data, the neotectonic movements and the general structural setting (Amodio Morelli et al., 1976; Ghisetti and Vezzani, 1979; De Vivo et al., 1979). According to these last authors, the maximum possible earthquake magnitude has been estimated to be 7.4, which is somewhat higher than the Messina (1908) and Pizzo Calabro (1905) catastrophic events having *M* values of 7.0 and 7.3, respectively (Kárník, 1969). The region is formed by a mountainous, narrow belt which divides the Tyrrhenian Sea

\* Progetto Finalizzato Geodinamica, C.N.R., Publication No. 465.

and the Ionian Sea, two deep basins characterized by high values (respectively 260 and 310 mGal) of Bouguer gravity anomalies. The Aeolian Islands, emerging in the south-eastern Tyrrhenian Sea, are part of a young calc-alkaline volcanic district located between the Calabrian–Sicilian coast and the bathyal plain.

The whole Tyrrhenian region is characterized by anomalous seismic wave propagation, with high attenuation of S waves in the mantle and in the crust, and with early arrivals of P waves at seismic stations located in southern Italy. Seismic characteristics suggest the presence of a high-velocity body in the mantle (Caputo et al., 1972; Del Pezzo et al., 1979). Intermediate and deep earthquakes have been observed in this region since the early work by Gutenberg and Richter (1948). The activity is mostly concentrated between 250 and 340 km depth, with a few earthquakes between 400 and 500 km (Caputo and Postpischl, 1973; Ritsema, 1979). Focal mechanisms of intermediate earthquakes reported in the literature indicate maximum pressure axes ( $P$ ) plunging  $60^\circ$  in a WNW direction, parallel to the dip of the Benioff zone, and tension axes ( $T$ ) oriented ESE with  $30^\circ$  dip (Ritsema, 1972). A gap is usually reported between 100 and 200 km depth, in agreement with the asthenospheric low-velocity zone inferred from surface wave dispersion measurements (Panza, 1979). The reduced activity below 340 km depth also coincides with a zone of P-wave velocity reversal (Mechler and Mseddi, 1977).

The physiographical, geophysical and volcanological characteristics of the Southern Tyrrhenian area suggest that the Calabrian arc may be considered a Mediterranean counterpart of the Pacific island arcs, and the Tyrrhenian Sea a counterpart of the Pacific marginal basins (Boccaletti and Guazzone, 1972; Barberi et al., 1977). However, the Calabrian arc is quite different from the Pacific subduction zones, both in size and structural context (Scandone, 1979; Calcagnile et al., 1981). It is located in the center of the Mediterranean area, where continent–continent collision between the African and European plates already occurred at the end of the Eocene, so that the previous Tethian oceanic lithosphere was consumed before 40 Ma ago. It follows that a lot of continental lithosphere had to be involved in the subduction processes which resulted in the development of the Maghrebic and Apenninic nappes (Scandone, 1979). The great depth reached by the earthquake hypocenters (480 km) suggests that subduction took place over a long time. It is noteworthy that the rates inferred from seismic moments of earthquakes (McKenzie, 1972), mass conservation across the Eurasia–Africa plate boundary (Le Pichon et al., 1973) and regional palinspastic restorations (Scandone et al., 1974) do not show great differences, ranging from 1.4 cm/y to 2.5 cm/y.

In this paper the space distribution of the intermediate and deep earthquakes is examined and a new set of fault-plane solutions is evaluated and compared to those reported by Cagnetti et al. (1978). A reconstruction of the present stress field is then attempted, in order to arrive at details of the stress pattern expected in an area of continent–continent collision, where subduction has been going on at least until the Pliocene. The kinematics of the region, moreover, is complicated by the opening of

the Tyrrhenian basin which cannot be fully explained by classical marginal basin models.

#### DATA ANALYSIS

The catalogue of deep and intermediate earthquakes of the southern Tyrrhenian region includes about 100 events since 1910 (Fig. 1 and Table 1). The epicenters lie within a small area extending from northern Sicily to  $41^\circ\text{N}$ , the deepest events being located in the center of the Tyrrhenian Sea, just below the bathyal plain. A few events have been located in the Ionian Sea, between 50 and 70 km depth, with the aid of later arrivals (pP-P phases). Since 1975, about 15 earthquakes have been located in the triangle formed by southern Calabria, northern Sicily and the Aeolian Islands, between 100 and 200 km depth, using data from the improved local seismic network. The hypocenter distribution, derived from ISC and NOAA Bulletins, allows us to define a lithospheric body plunging NW with an average dip of  $45^\circ$  (Figs. 2 and 3). This peculiar Benioff zone has a concave shape and an arc-like structure with almost vertical dipping as far as 250 km depth, a  $50^\circ$  dip from 250 to 340 km depth, and a quasi-horizontal dipping for greater depths. The structure is

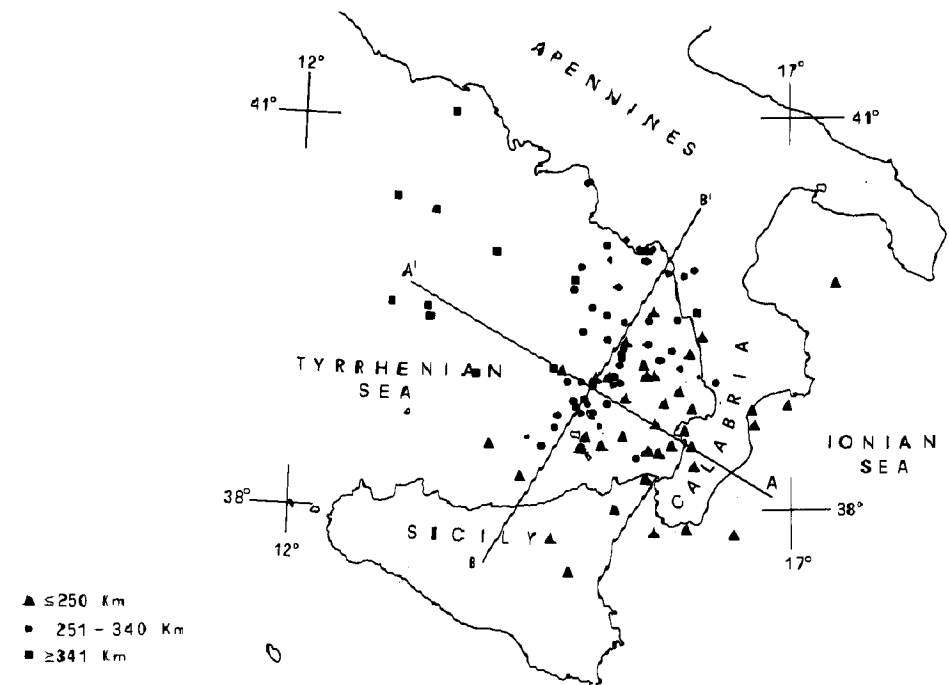


Fig. 1. Epicenter map of deep and intermediate earthquakes which occurred in southern Italy in the period 1910–1979.

TABLE I

List of intermediate and deep earthquakes of the Calabrian arc. Magnitude values are from Kárník (1969) in the period 1910–1955, from Rothé (1969) in the period 1956–1963 and in later years ISC and NEIS  $m_B$  values are reported

No.	Date	Origin time	Lat. N	Long. E	Depth (km)	$M$	Source *
1	1.08.1910	10:40:24	39	15	200	6.8	ISS
2	5.04.1911	15:28:12	40	15.5	200	6.3	ISS
3	7.07.1915	16:42:48	39	15	275	5.9	ISS
4	17.08.1926	01:42:53	39	14.75	100	6.0	ISS
5	7.03.1928	10:55:02	38.5	16.0	100	6.6	ISS
6	17.10.1937	09:59:09	39.0	15.2	300	5.8	ISS
7	13.04.1938	02:45:46	39.36	15.50	270	7.1	ISS
8	17.09.1943	03:39:20	39.5	15.5	270	5.5	ISS
9	3.04.1946	17:01:44	39.8	160	319	4.2	ISS
10	26.02.1947	05:42:06	39.0	15.2	276	5.0	ISS
11	31.07.1947	07:54:52	39.25	15.25	290	5.6	ISS
12	1.09.1947	22:18:54	39.25	15.25	250	5.2	ISS
13	10.09.1952	04:17:06	39.0	15.2	223	5.3	ISS
14	26.12.1952	23:55:57	39.9	15.5	287	6.2	ISS
15	30.07.1953	11:52:57.1	39.0	16.2	280	5.0	ISS
16	23.11.1954	13:00:05.5	38.6	15.1	239	5.3	ISS
17	17.02.1955	19:31:33	39.6	13.3	438	5.6	ISS
18	1.02.1956	15:10:50.6	39.03	15.63	234	6.2	DP
19	5.01.1957	18:48:10	38.5	14.5	306	5.3	DP
20	20.05.1957	19:57:35	38.5	14	60	5.8	DP
21	23.12.1959	09:29:03	37.72	14.61	77	5.3	DP
22	3.10.1960	20:19:34	39.26	15.29	283	6.2	ISS
23	25.03.1962	21:38:26	39.12	14.55	343	5.3	ISS
24	1.06.1963	20:36:05	38.65	14.93	250	4.4	ISC
25	26.07.1963	09:26:46.4	39.6	15.2	337	4.2	ISC
26	14.04.1964	06:35:27.0	38.84	14.78	293	4.3	ISC
27	4.10.1964	01:46:50.4	39.12	15.45	242	4.6	ISC
28	12.03.1965	20:19:08.0	38.8	17.6	95	4.5	ISC
29	19.12.1965	09:14:17.6	39.4	16.1	230	4.1	NEIS
30	23.12.1965	15:29:06.9	40.53	14.87	310	4.6	ISC
31	3.02.1966	13:23:28.5	38.51	14.89	242	4.3	ISC
32	14.02.1967	14:42:26.2	38.45	15.45	258	4.2	ISC
33	2.06.1967	20:20:23.9	38.81	14.95	283	4.1	ISC
34	7.09.1967	14:09:03.6	37.85	15.94	53	4.4	ISC
35	21.04.1968	21:09:48.0	39.82	14.88	320	4.1	ISC
36	1.10.1968	16:31:03.2	40.19	15.30	295	4.3	ISC
37	29.03.1969	01:43:38.7	40.04	15.10	310	4.6	ISC
38	2.04.1969	01:38:02.1	38.98	15.24	263	4.7	ISC
39	13.04.1969	05:45:43.4	38.82	14.84	275	4.1	ISC
40	15.04.1969	00:56:52.8	39.69	14.95	319	4.0	ISC
41	12.10.1969	18:54:35.4	39.91	15.17	306	4.0	ISC

TABLE I (continued)

No.	Date	Origin time	Lat. N	Long. E	Depth (km)	$M$	Source *
42	23.10.1969	02:12:47.9	38.51	15.27	244	4.2	ISC
43	8.12.1969	04:44:20.2	39.46	15.58	247	4.0	ISC
44	11.12.1969	06:00:55.2	39.39	14.85	295	4.1	ISC
45	29.01.1970	11:09:24.5	38.75	14.83	284	4.6	ISC
46	17.02.1970	07:32:02.6	39.83	15.92	273	4.1	ISC
47	2.04.1970	21:26:39.5	38.29	14.28	226	4.6	ISC
48	5.06.1970	09:20:56.1	39.18	15.54	267	4.3	ISC
49	29.06.1970	14:22:53.9	38.72	16.66	69	4.6	ISC
50	16.08.1970	10:45:22.1	37.88	16.46	53	4.3	ISC
51	3.04.1971	04:03:56.5	38.86	15.10	283	4.1	ISC
52	25.04.1971	04:39:28.9	39.30	15.26	293	4.4	ISC
53	1.05.1971	22:20:10.6	39.67	15.29	292	4.1	ISC
54	21.08.1971	03:59:04.2	39.65	12.90	485	4.1	ISC
55	9.11.1972	11:47:16	40.3	13.3	455		ISC
56	17.05.1973	20:43:13.0	39.28	15.96	127		ISC
57	11.08.1973	23:53:01.0	39.93	14.00	423		ISC
58	13.12.1973	01:57:06	39.8	15.64	274		ISC
59	20.12.1973	17:44:25.5	38.76	14.80	267	4.9	ISC
60	10.01.1974	11:53:33	38.86	14.83	337	4.0	ISC
61	21.01.1974	20:11:56	38.90	15.26	100	3.8	ISC
62	24.01.1974	13:19:23.4	39.85	14.58	360	4.2	ISC
63	22.07.1974	07:19:32.7	39.25	15.38	257	4.5	ISC
64	16.09.1974	22:22:41.8	38.55	15.58	83		ISC
65	21.10.1974	14:49:25.9	39.50	15.31	296	4.8	ISC
66	31.01.1975	20:19:58	39.70	17.40	69		ISC
67	12.04.1975	16:47:03.4	38.45	15.56	178	4.2	ISC
68	4.05.1975	21:27:55.1	39.47	13.37	438		ISC
69	30.07.1975	03:01:15.1	37.53	14.83	60		ISC
70	10.08.1975	20:55:50.9	38.53	15.60	197	4.6	ISC
71	23.08.1975	17:42:53.5	39.48	15.76	267	3.8	ISC
72	30.09.1975	07:50:35.0	39.67	14.90	303	3.7	ISC
73	5.11.1975	07:46:28.8	38.59	15.93	113	4.1	ISC
74	18.12.1975	13:13:19.0	38.80	15.78	189	4.0	ISC
75	6.04.1976	09:08:58.2	38.75	16.07	110	4.8	ISC
76	12.08.1976	06:18:06	37.8	15.6	144		ISC
77	21.09.1976	15:01:50.0	38.74	14.68	296	4.7	ISC
78	20.06.1977	02:04:10.6	39.21	15.70	260	4.2	ISC
79	28.06.1977	07:12:49.0	38.60	14.70	260	5.0	ISC
80	15.08.1977	21:10:32.5	38.79	17.03	74	4.9	ISC
81	20.12.1977	20:04:14.7	38.44	15.70	169	4.7	ISC
82	25.12.1977	02:11:11.3	40.42	12.95	481	4.5	ISC
83	30.12.1977	17:35:08.9	39.98	15.45	270	5.4	ISC
84	30.12.1977	18:08:50.7	39.94	15.45	292	4.7	ISC
85	6.02.1978	16:27:24.7	38.80	15.00	300	3.6	ISC
86	29.04.1978	23:49:22.9	39.03	13.84	431	4.2	ISC

TABLE I (continued)

No.	Date	Origin time	Lat. N	Long. E	Depth (km)	<i>M</i>	Source *
87	23.05.1978	08:13:24.0	38.00	15.20	182	3.4	ISC
88	25.06.1978	15:36:55.2	39.09	15.65	241	4.0	ISC
89	9.08.1978	09:08:58.8	38.27	15.55	192	3.5	ISC
90	13.08.1978	16:53:46.4	38.41	16.01	137	4.2	ISC
91	27.12.1978	17:46:10.4	41.08	13.56	391	5.4	ISC
92	22.03.1979	19:32:44.7	38.81	15.85	114	4.7	NEIS
93	25.03.1979	11:36:26.2	39.44	15.21	306	4.5	NEIS
94	25.07.1979	00:18:12.5	39.22	15.90	310	4.3	CSEM
95	21.09.1979	23:47:37.0	39.07	14.74	317	4.6	NEIS
96	23.09.1979	05:51:33.3	39.61	16.06	385		NEIS

\* CSEM=Centre Seismologique Européo-Mediterranéen, DP=De Panfilis, 1958. Attività sismica in Italia 1953-1957, Ann. Geofis., XII, 1, ISC=Bulletin of the International Seismological Centre, ISS=International Seismological Summary, NEIS=National Earthquake Information Service.

almost continuous in the central part of the Calabrian arc, while it is less defined northward, between latitude  $40^{\circ}$ – $41^{\circ}$ N; in the south the structure appears to be sharply interrupted west of the Aeolian Islands. Most of the earthquake energy has been released in the zone of maximum concavity in the 250–340 km depth range, where on April 13th, 1938 an earthquake with  $M = 7.1$  occurred.

Hypocenter coordinates of deep and intermediate earthquakes in the Tyrrhenian Sea have been relocated by using the Joint Hypocenter Determination (JHD) technique. This method allows us to locate simultaneously a group of earthquakes, and to estimate the station corrections by minimizing the sum of squared residuals at receiving seismic stations. The method is extensively used (Douglas, 1967; Dewey, 1972; Qamar, 1974; Cardwell and Isacks, 1976), allowing, in general, an improvement of the bias in the hypocenter location caused by lateral velocity variations and missing stations. Although it is applied only to a relatively small number of stations, the recent technique developed by Frohlich (1979) permits the use of a quite large number of stations/events. A number of seismic stations, varying between 50 and 100, have been utilized to relocate the earthquakes in the Tyrrhenian Sea, and the data have been selected in three intervals, according to their depth. Those earthquakes which occurred since 1962 have been relocated (Table II); in the period preceding 1962 the scattering is somewhat higher, due to the scarcity and relatively poor quality of the data. The observed shift between the hypocenters evaluated by the JHD method with respect to the traditional ISC location is not more than 10 km on average.

As shown in Fig. 4, the scattering in the hypocenter alignment is reduced from 100 to about 50 km. However the depth control is not yet satisfactory, and only the

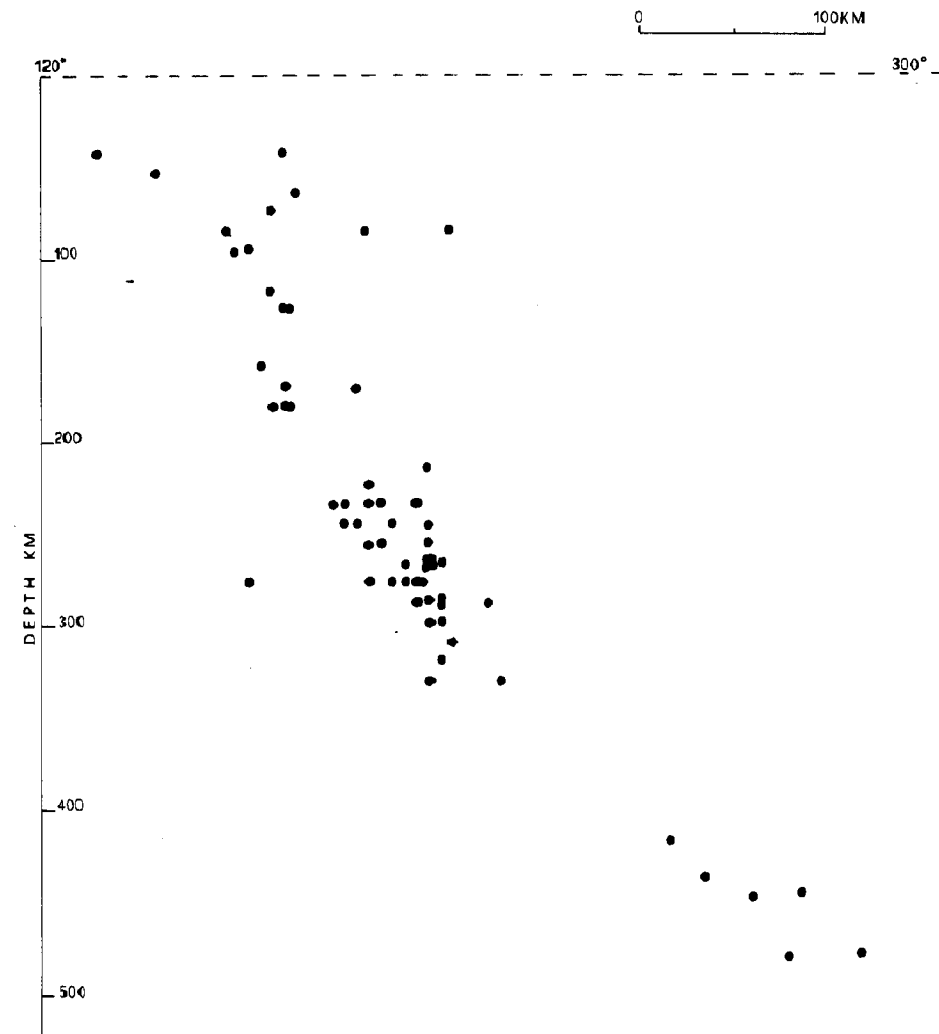


Fig. 2. Distribution of intermediate and deep hypocenters along the line AA' of Fig. 1. Only earthquakes with horizontal distance less than 50 km from the line are included.

use of depth phases, in the absence of a good station distribution and an appropriate velocity model, could reduce the systematic hypocenter mislocations.

#### FAULT-PLANE SOLUTIONS

All the data on the P-wave first motions, available in the appropriate bulletins and a great number of seismograms, have been analysed in order to determine the

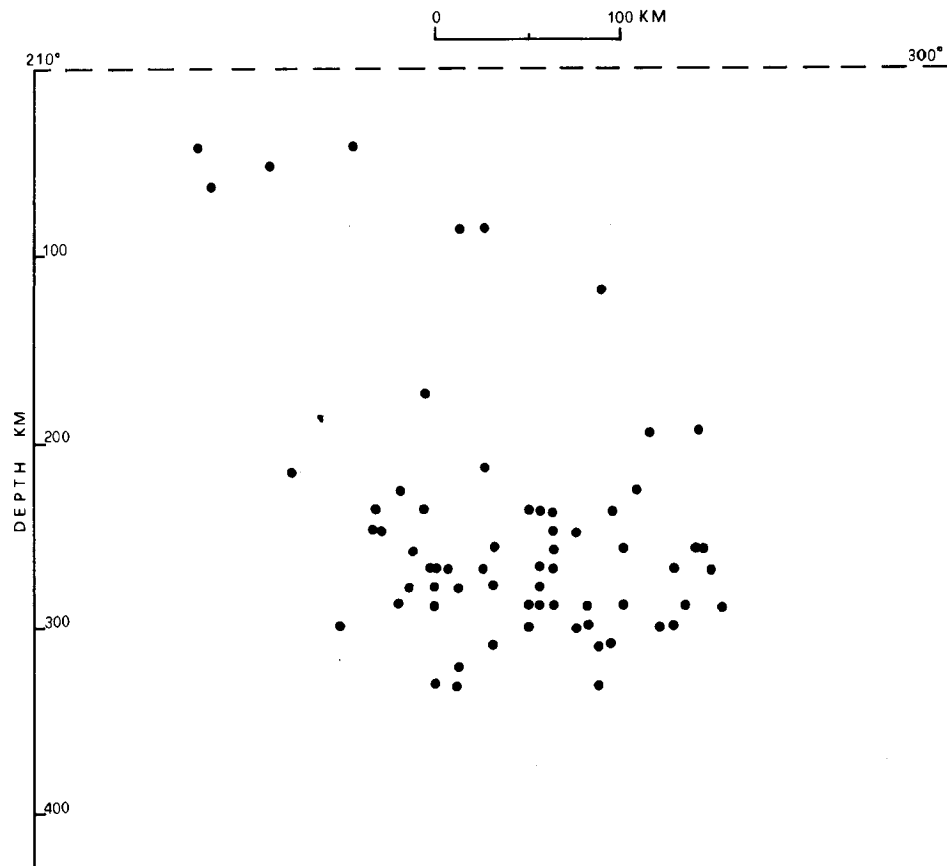


Fig. 3. Same as Fig. 2, along the line  $BB'$  of Fig. 1.

fault-plane solutions of earthquakes which occurred in the Calabrian arc and the surrounding regions.

Due to the large amount of data, fault-plane solutions have been estimated through a slightly modified version of the Wickens and Hodgson (1967) computer program. The method consists of searching numerically for the maximum of the function, called score:

$$\text{SCORE} = \left| \frac{\sum W_{pi} \text{sgn } \phi_i \text{sgn } R_i \pm D}{\sum |W_{pi}|} \right|$$

where  $\text{sgn } \phi_i$  and  $\text{sgn } R_i$  are, respectively, the theoretical and observed signal polarities, and  $W_{pi}$  is a weighting function according to Knopoff (1961). The term  $D$  is based on the sign change between adjacent trial positions and it is introduced in the numerical searching process to emphasize maxima of the score. In our program,

TABLE II

Hypocenters relocated by the JHD method

Date	Origin time	Lat. N	Long. E	Depth (km)
12.04.1975	16:47:02.5±0.7	38.38±0.07	15.51±0.09	165±11
10.08.1975	20:55:50.1±0.7	38.47±0.08	15.54±0.09	186±13
05.11.1975	07:46:28.3±1.0	38.52±0.14	15.93±0.12	110±18
18.12.1975	13:13:18.2±1.0	38.82±0.12	15.62±0.14	198±16
06.04.1976	09:08:57.3±1.1	38.65±0.16	16.02±0.12	102±20
12.08.1976	06:17:58.4±0.1	36.78±0.01	15.07±0.02	182±1
20.12.1977	20:04:14.4±0.9	38.44±0.10	15.55±0.13	172±17
13.08.1978	16:53:47.9±0.5	38.67±0.06	15.91±0.05	115±6
09.08.1978	09:08:59.1±0.7	38.39±0.09	15.32±0.08	195±10
25.03.1962	21:37:59.4±1.2	39.12±0.13	14.49±0.25	338±19
01.06.1963	20:35:59.0±1.1	38.62±0.12	14.89±0.20	260±16
14.04.1964	06:35:23.9±0.6	38.67±0.06	14.72±0.13	282±9
04.10.1964	01:46:49.3±0.8	39.09±0.08	15.44±0.14	252±12
23.12.1965	15:29:03.4±0.9	40.36±0.10	14.90±0.16	295±13
03.02.1966	13:23:27.5±0.8	38.51±0.09	14.89±0.18	251±13
14.02.1967	14:42:26.0±0.9	38.49±0.09	15.10±0.20	265±17
02.06.1967	20:20:20.7±0.5	38.65±0.05	14.88±0.09	268±9
21.04.1968	21:09:46.1±0.4	39.76±0.05	14.84±0.07	316±7
01.10.1968	16:31:01.2±0.6	40.12±0.06	15.35±0.09	289±10
29.03.1969	01:43:36.5±0.8	39.95±0.10	15.05±0.12	309±13
13.04.1969	05:45:42.0±1.1	38.79±0.12	14.87±0.18	287±17
15.04.1969	00:56:51.1±0.6	39.64±0.07	14.87±0.11	320±10
12.10.1969	18:54:33.7±0.4	39.84±0.05	15.13±0.05	309±8
23.10.1969	02:12:47.2±0.8	38.58±0.09	15.25±0.12	252±11
08.12.1969	04:44:17.7±0.4	39.28±0.05	15.53±0.06	247±10
29.01.1970	11:09:22.4±0.7	38.67±0.08	14.83±0.11	283±13
17.02.1970	07:32:01.0±0.5	39.80±0.05	15.81±0.09	269±8
05.06.1970	09:20:54.6±0.7	39.12±0.08	15.49±0.10	266±12
03.04.1971	04:03:54.8±0.6	38.76±0.06	14.95±0.10	280±10
25.04.1971	04:39:27.5±0.8	39.22±0.09	15.21±0.12	294±13
01.05.1971	22:20:08.6±0.8	39.56±0.09	15.19±0.12	284±16
20.12.1973	17:44:23.7±0.8	38.72±0.09	14.79±0.12	265±15
24.01.1974	13:19:21.2±1.0	39.74±0.12	14.49±0.13	357±20
22.07.1974	07:19:30.8±0.8	39.14±0.09	15.32±0.11	261±15
21.10.1974	14:49:23.9±0.7	39.37±0.08	15.21±0.10	291±15
23.08.1975	17:42:53.4±1.1	39.57±0.12	15.82±0.14	266±22
30.09.1975	07:50:30.3±1.0	39.29±0.11	15.17±0.12	339±40
21.09.1976	15:01:48.3±0.6	38.69±0.06	14.64±0.09	302±12
20.06.1977	02:04:10.0±0.9	39.20±0.10	15.77±0.12	261±17
28.06.1977	07:12:47.3±0.8	38.53±0.09	14.69±0.12	262±15
30.12.1977	17:35:07.2±0.7	39.90±0.08	15.35±0.10	290±14
30.12.1977	18:08:49.3±0.6	39.88±0.08	15.38±0.08	292±14
25.06.1978	15:36:55.3±0.8	39.18±0.09	15.63±0.12	240±17
21.08.1971	03:59:04.2±0.6	39.66±0.08	12.82±0.11	488±14

TABLE II (continued)

Date	Origin time	Lat. N	Long. E	Depth (km)
09.11.1972	11:47:08.1±0.7	39.71±0.08	13.84±0.11	426±17
11.08.1973	23:52:59.8±1.1	39.85±0.13	13.80±0.17	418±21
24.01.1974	13:19:23.7±0.6	39.88±0.07	14.53±0.09	365±14
04.05.1975	21:27:54.0±0.3	39.36±0.03	13.58±0.05	455±14
25.12.1977	02:11:11.5±0.4	40.42±0.05	12.96±0.07	475±11
29.04.1978	23:49:24.2±0.5	39.23±0.06	13.87±0.08	424±18
27.12.1978	17:46:10.7±0.5	41.14±0.06	13.49±0.06	397±12

a plot of the solutions having the best score is systematically made in order to control the major differences between solutions having the same number of inconsistent polarity readings. Data have been plotted on a lower hemisphere Wulff projection. Incidence angles at the focus have been calculated from the Herrin et al. (1968) travel-time tables, from all distance ranges available.

From an initial set of solutions relating to about 100 earthquakes, 59 focal mechanisms have been selected according to their reliability, i.e. to the number of azimuthal coverage of first motions of the percentage of discarding points with respect to a double couple source model.

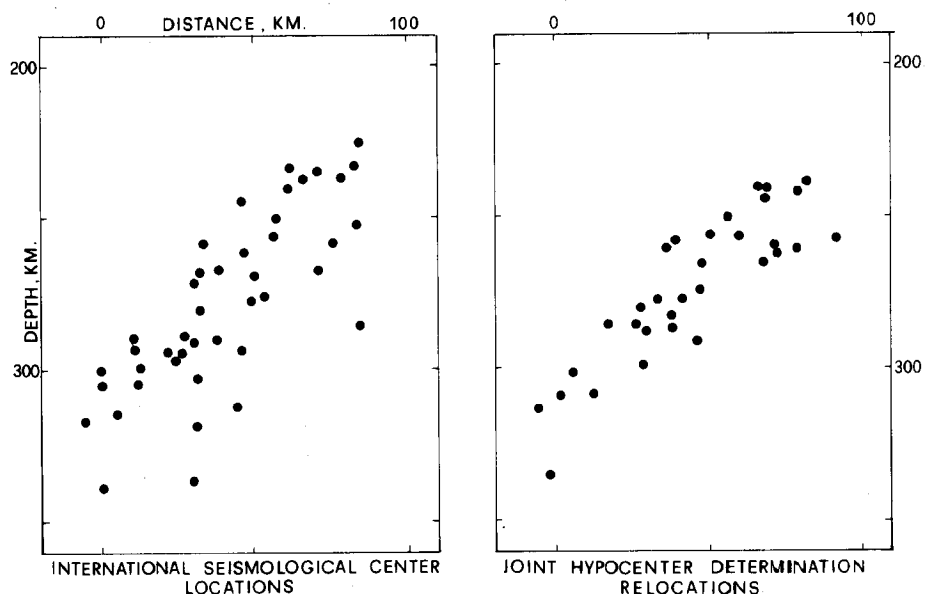


Fig. 4. Comparison of hypocenters listed in the ISC Bulletin with those relocated through Joint Hypocenter Determination. The projection is along the line AA'.

The 59 reliable fault-plane solutions related to the shallow and intermediate earthquakes that occurred in southern Italy in the period 1908–1980, are reported in Figs. 5, 6 and Table III. The focal mechanisms of earthquakes located in the concave part of the slab show a predominance of down dip compression, mostly parallel to the dip of the Benioff zone, in agreement with the results available in the literature (Ritsema, 1972; Riuscetti and Schick, 1975). In addition, the earthquakes in the northern and southern parts of the slab reveal a predominance of strike-slip motions, supporting the hypothesis of lateral bending of the arc. North of the Messina Strait, focal mechanisms of intermediate earthquakes show *P* axes trending ENE–WSW, almost parallel to the strike of the Benioff zone. This fact may be accounted for by the strong curvature of the Benioff zone that can produce compression in the inner part of the arc and stretching in the outer part, which has been observed in many other regions (Strobach, 1973; Richter and Strobach, 1978). The catastrophic Messina earthquake of 1908 ( $M = 7.0$ ) can easily be explained by lateral stretching of the crust in the outer part of the arc.

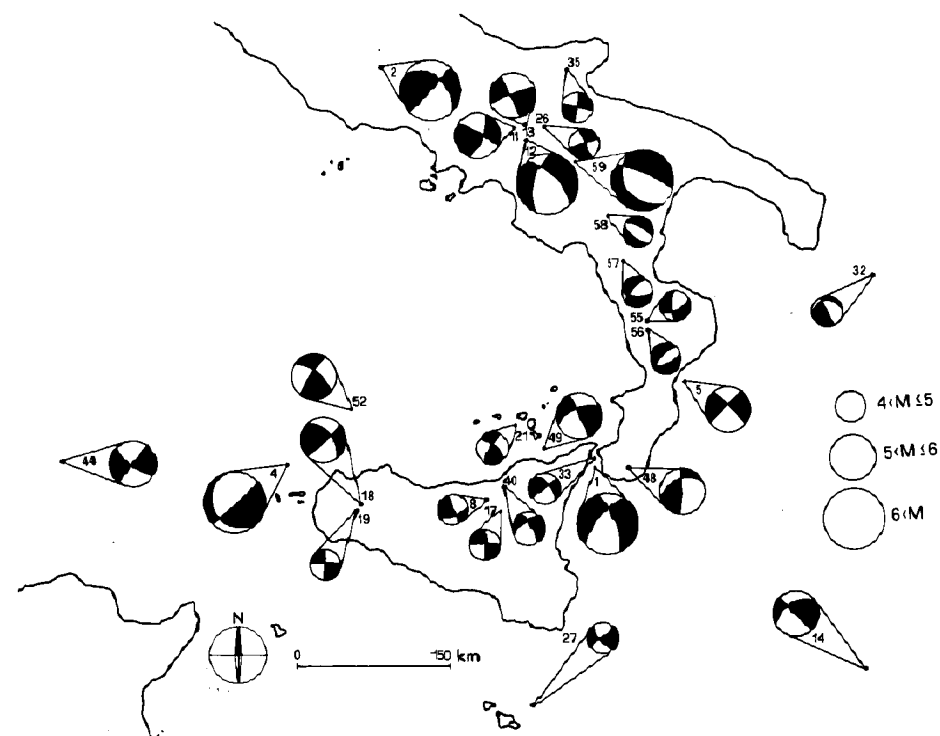


Fig. 5. Most reliable fault-plane solutions of crustal earthquakes located along the Calabrian arc and surrounding regions. Data are projected on a Wulff net, lower hemisphere. Black and white areas are compressive and dilatational quadrants, respectively.

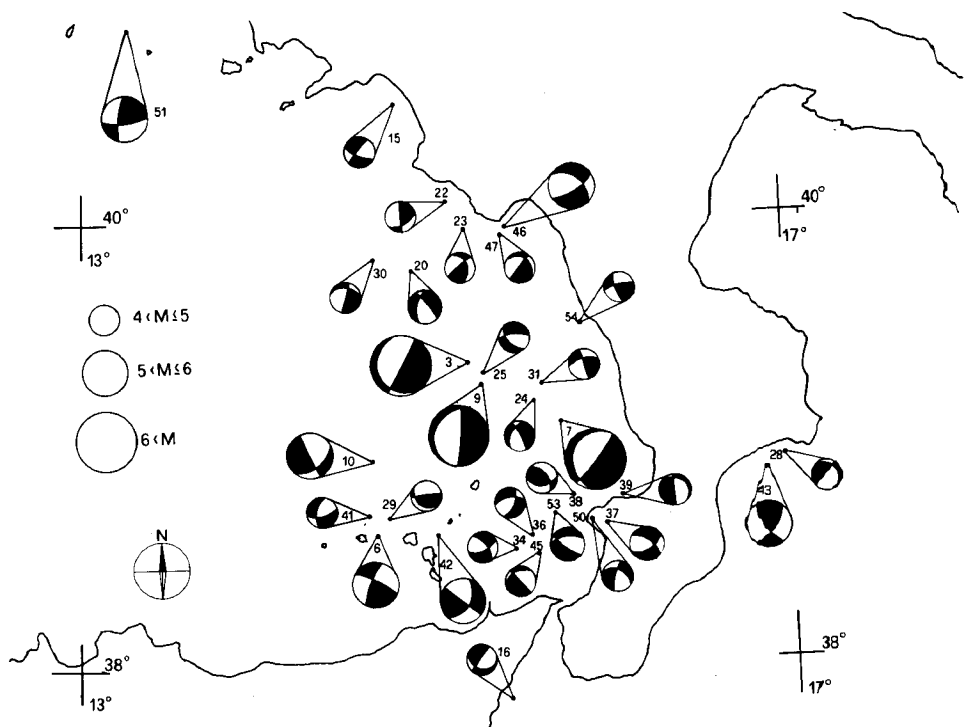
TABLE III  
Focal-mechanism solutions

No.	Date		Lat. N	Long. E	<i>H</i>	<i>M</i>
1	28.12.1908	04:20	38.12	15.60	10	7.0
2	13.01.1915	06:52	41.83	13.43	8	6.8
3	13.04.1938	02:45	39.36	15.50	270	7.1
4	16.03.1941	16:35	38.44	12.12	20	6.9
5	11.05.1947	06:22	38.69	16.78	14	5.6
6	23.11.1954	13:00	38.6	15.1	239	5.3
7	01.02.1956	15:10	39.03	15.63	234	6.2
8	23.12.1959	09:29	37.72	14.61	77	5.3
9	03.01.1960	20:19	39.26	15.29	283	6.2
10	25.03.1962	21:38	39.12	14.55	343	5.3
11	21.08.1962	18:09	41.23	15.01	25	5.7
12	21.08.1962	18:19	41.25	15.05	28	6.1
13	21.08.1962	18:44	41.18	15.09	36	6.0
14	29.09.1963	22:16	36.00	18.08	37	5.7
15	23.12.1965	15:29	40.53	14.87	310	4.6
16	07.09.1967	14:09	37.85	15.94	53	4.4
17	31.10.1967	21:08	37.84	14.60	38	5.0
18	15.01.1968	01:33	37.89	13.08	20	5.1
19	25.01.1968	09:56	37.71	13.06	4	5.0
20	21.04.1968	21:09	39.82	14.88	320	4.1
21	19.05.1968	09:37	38.52	14.82	39	4.8
22	29.03.1969	01:43	40.04	15.10	310	4.6
23	02.04.1969	01:38	38.98	15.24	263	4.7
24	05.06.1970	09:20	39.18	15.54	267	4.3
25	25.04.1971	04:39	39.30	15.26	293	4.4
26	06.05.1971	03:45	41.20	15.24	33	4.8
27	21.03.1972	23:06	35.80	14.98	5	4.5
28	13.04.1973	08:12	38.97	16.92	43	4.5
29	20.12.1973	17:44	38.76	14.80	267	4.9
30	24.01.1974	13:19	39.85	14.58	360	4.2
31	22.07.1974	07:19	39.25	15.38	257	4.5
32	23.11.1974	18:46	39.74	18.94	49	4.7
33	16.01.1975	00:09	38.14	15.71	21	4.6
34	12.04.1975	16:47	38.45	15.56	178	4.2
35	19.06.1975	10:11	41.65	15.73	18	4.9
36	10.08.1975	20:55	38.53	15.60	197	4.6
37	05.11.1975	07:46	38.59	15.93	113	4.1
38	18.12.1975	13:13	38.80	15.78	189	4.0
39	06.04.1976	09:08	38.75	16.07	110	4.8
40	17.09.1976	01:23	37.92	14.57	33	4.4
41	21.09.1976	15:01	38.74	14.68	296	4.7
42	28.06.1977	07:12	38.60	14.70	260	5.0

Plane A		Plane B		P axis		T axis		B axis	
strike	dip	strike	dip	trend	plunge	trend	plunge	trend	plunge
169	42	208	55	173	68	281	7	13	20
34	85	118	39	154	29	270	38	38	39
30	89	125	16	315	44	105	42	209	16
166	15	52	84	337	50	130	37	230	14
122	68	206	77	162	25	255	6	358	65
117	64	196	69	248	4	156	34	343	56
8	13	215	79	312	56	120	33	213	6
97	27	162	78	53	29	280	51	156	24
6	77	179	14	278	59	95	32	185	2
42	16	147	86	41	47	251	39	148	16
32	65	118	81	347	11	252	24	99	64
134	70	192	34	187	56	65	20	324	27
164	69	257	2	29	9	123	21	277	68
137	87	235	22	207	38	68	44	315	22
100	54	202	74	67	38	328	13	222	46
46	85	116	16	121	48	329	38	227	15
9	61	93	80	227	28	324	13	76	60
40	82	122	46	163	23	272	37	48	45
4	89	94	79	230	8	138	9	1	79
158	72	187	21	233	62	76	26	341	10
18	67	133	45	260	13	154	50	1	37
54	8	358	86	274	40	81	49	178	7
190	27	226	67	304	21	162	64	39	15
157	78	192	15	235	57	74	32	338	9
261	45	298	50	91	70	190	3	281	20
162	84	252	86	297	2	207	7	39	83
236	76	86	67	65	6	100	27	264	63
31	89	67	3	124	44	299	46	31	3
82	80	125	14	360	34	160	54	263	10
14	79	45	13	276	56	110	33	15	7
64	40	162	84	217	38	103	27	347	40
95	7	337	87	74	48	241	41	336	7
62	85	152	58	192	19	292	26	70	58
160	69	68	86	296	12	202	16	58	69
101	72	15	79	147	5	240	21	45	69
217	55	275	53	247	57	155	1	64	34
126	63	75	39	260	61	15	13	111	26
167	50	52	63	23	7	283	51	118	39
28	7	266	87	92	44	261	41	355	6
142	69	200	36	194	56	333	28	74	19
85	67	187	64	45	25	137	2	229	55
41	37	137	85	15	39	257	30	141	47

TABLE III (continued)

No.	Date		Lat. N	Long. E	<i>H</i>	<i>M</i>
43	15.08.1977	21:10	38.79	17.03	74	4.9
44	28.08.1977	09:45	38.21	8.21	10	5.1
45	20.12.1977	20:04	38.44	15.70	169	4.7
46	30.12.1977	17:35	39.98	15.45	270	5.4
47	30.12.1977	18.08	39.94	15.45	292	4.7
48	11.03.1978	19:20	38.10	16.03	33	5.6
49	15.04.1978	23:33	38.29	15.70	10	5.6
50	13.08.1978	16:53	38.41	16.01	137	4.2
51	27.12.1978	17:46	41.08	13.56	391	5.4
52	20.01.1979	13:49	38.87	12.86	4	5.2
53	22.03.1979	19:32	38.81	15.85	114	4.7
54	25.03.1979	11:36	39.44	15.21	306	4.5
55	20.02.1980	02:34	39.32	16.20	10	4.4
56	20.02.1980	02:40	39.33	16.19	10	4.3
57	09.03.1980	12:00	39.99	15.91	10	4.3
58	14.05.1980	01:40	40.36	15.77	15	4.2
59	23.11.1980	18:34	40.77	15.30	18	6.8



Plane A		Plane B		P axis		T axis		B axis	
strike	dip	strike	dip	trend	plunge	trend	plunge	trend	plunge
48	57	337	64	281	4	15	44	187	46
222	89	312	81	357	6	87	8	229	81
31	18	148	82	72	35	221	51	330	16
57	69	122	44	281	50	175	15	73	37
139	17	221	88	296	40	148	45	40	17
183	82	255	31	117	30	243	45	7	30
240	72	327	83	194	8	102	18	306	71
167	50	52	63	23	7	283	51	118	39
88	62	190	69	317	5	51	36	221	54
30	70	132	68	263	1	173	30	355	60
128	41	354	59	134	64	244	10	338	24
342	49	224	62	5	53	106	8	201	36
187	47	242	58	26	59	127	7	220	31
210	48	42	43	57	83	306	3	215	7
202	61	248	39	66	64	312	11	216	24
130	30	120	61	197	74	34	16	302	5
118	64	325	29	183	68	37	18	303	12

The motion inferred by the crustal fault-plane solutions is in general quite complex. *P* axes oriented WNW-ESE along the Ionian coast of Calabria are present both in the crust and in the uppermost part of the slab. In Sicily strike-slip fault mechanisms are predominant. North of the Calabrian arc, in the southern Apennines, mechanisms show predominant dip slip motions with *T* axes normal to the main structural trend of the chain and subordinate strike slip faults. Tension faulting in correspondence with the axis of the Apennines is interpreted as due to a sort of rift process which is presently migrating from the Tyrrhenian coast toward the crest of the mountain chain, producing progressive crustal thinning and consequent block faulting and foundering.

A schematic map showing the main structural elements of the Calabrian arc, the isobaths of the subducted slab and the observed stress field, as well as the preferred fault-plane orientation, is reported in Fig. 7.

Fig. 6. The most reliable fault-plane solutions of deep and intermediate earthquakes of southern Italy.



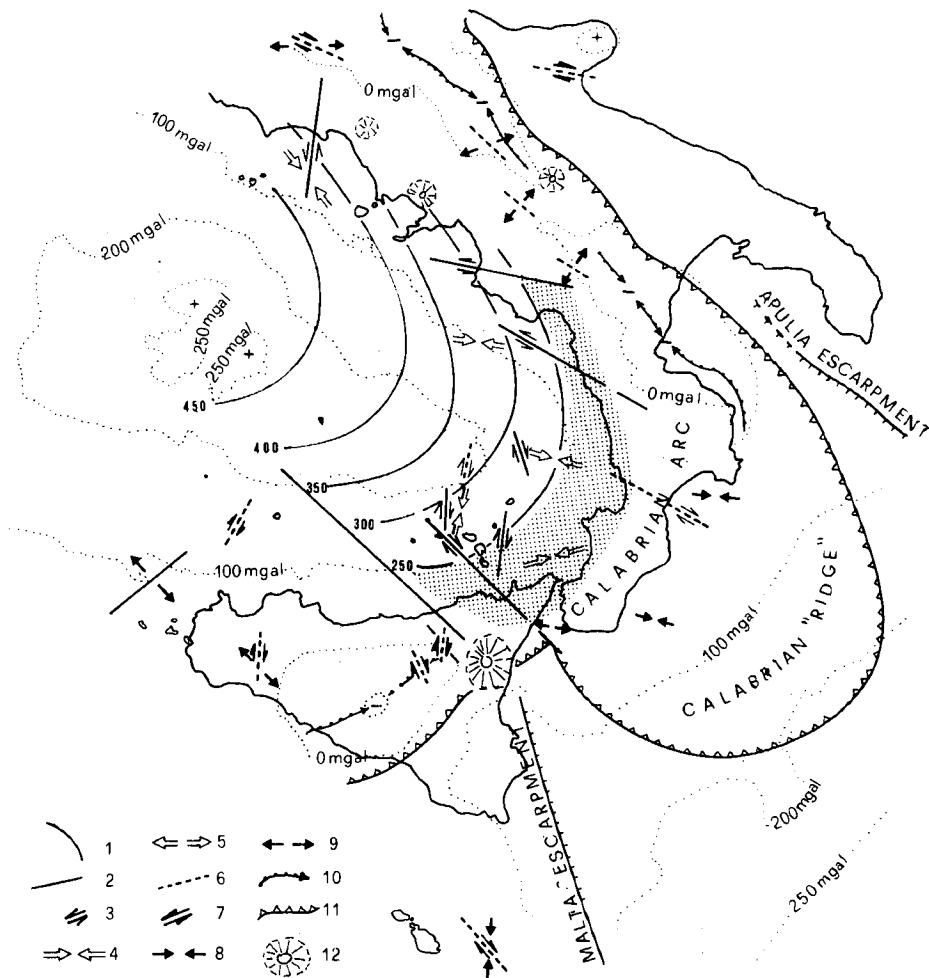


Fig. 7. Tectonic stress pattern and Bouguer anomalies of the Calabrian arc and surrounding regions. 1=isodepth contours of the Benioff zone, 2=deep faults deduced by focal mechanisms and consistent with crustal structure and the kinematic model, 3-5=strike slip, horizontal  $P$  and  $T$ -axes of intermediate and deep earthquakes, 6=hypothesized faults, 7-9=strike slip, horizontal  $P$  and  $T$ -axes of crustal earthquakes; 10=main dipping trend of gravimetric minima, 11=Neogene compressive front, 12=land quaternary volcanoes.

## DISCUSSION

The relocation of deep earthquake hypocenters by the JHD method represents an improvement with respect to the traditional determinations from bulletins, but the bias due to the source inhomogeneities revealed from the station residuals of local and teleseismic events (Scarpa, 1982) is still a relevant factor that may cause

systematic variations of hypocenter determinations and fault-plane solutions. The velocity contrast between the lithospheric slab and the surrounding mantle has been estimated to be approximately 10%. Notwithstanding such restrictions, the presently re-evaluated hypocenters and fault-plane solutions furnish considerable details on the complicated geometry of the Benioff zone and are an important contribution to the understanding of the dynamics of the Tyrrhenian area. In the first instance, the concentration of earthquake energy in the most concave part of the arc at 250-340 km depth can be better explained in terms of rheological properties of the subducted lithosphere than by plate detachment as it can be deduced from the almost continuous occurrence of earthquakes above the magnitude threshold typical of the seismic detection in the area in the last years ( $m_B \geq 3.5$ ).

The area of major continuity in the occurrence of intermediate and deep earthquakes closely corresponds to the area of maximum concavity, i.e. with the zone of maximum distortion of the arc. This zone may be interpreted as a strongly deformed remnant of a previously continuous Benioff zone extending during Oligocene time from the Northern Apennines to Gibraltar. This ancient Benioff zone was then sliced by strike-slip lithospheric faulting and was partly consumed in the asthenosphere as a consequence of the opening of the Western Mediterranean basin and the Tyrrhenian Sea. Towards the west, the last evidence of this old Benioff zone is provided by a few deep earthquakes which occurred in southern Spain.

In Fig. 8, a possible palinspastic restoration of the central Mediterranean area during Early Miocene time, i.e. before the opening of the Tyrrhenian Sea, is attempted. In this scheme the Tyrrhenian Sea did not open as a back-arc basin, but originated by a sort of rifting within the Alps-Apennine orogenic belt, followed by new lithosphere accretion. A calc-alkaline district was effectively present before the opening of the Tyrrhenian Sea, but it did not correspond to the Aeolian Islands, since its location was along the western margin of the Corsica-Sardinia block.

According to this hypothesis, the opening of the Tyrrhenian basin was accompanied during Late Miocene by an anticlockwise rotation of the Italian peninsula, which caused additional distortion of the Calabrian arc with consequent compression in the inner side of the arc and lateral stretching in the outer side. The recent calc-alkaline district of the Aeolian Islands may be related to a subduction renewal or to reactivation of the slab caused by the oroclinal distortion. The non-existence of a trench and the lack of negative free-air gravity anomalies along the Ionian side of the Calabrian arc would favour the second hypothesis.

The sketched model (Scandone, 1979) seems to fit the geological constraints in the landmasses and in the explored part of the sea, the magmatological implications, the neotectonic evidence and the earthquake fault-plane solutions. Following this model, in the Tyrrhenian Sea and in the Calabrian arc the classical model of arc-trench system migration may be rejected, while tremendous lithospheric distortion and tearings must have occurred after huge volumes of continental lithosphere were subducted during the collision of the Europe-Africa plates.

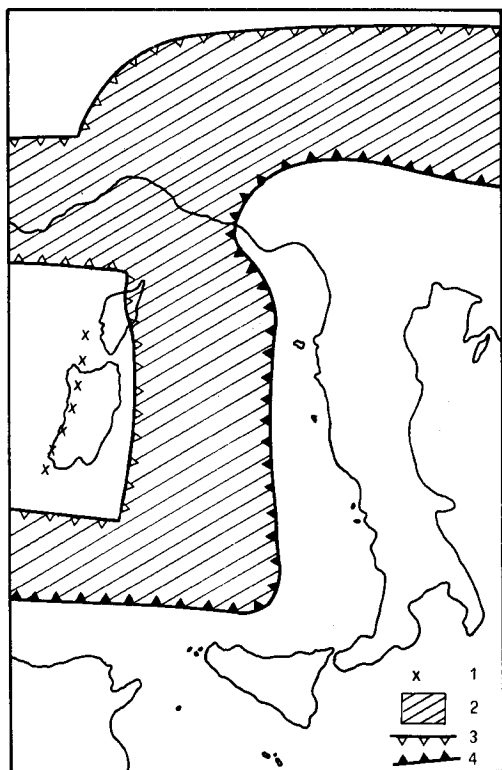


Fig. 8. Palinspastic restoration of the Central Mediterranean area during Early Miocene time (after Scandone, 1979). 1=Oligocene-Lower Miocene calc-alkaline district, 2=nucleus of Paleogene deformation between the European and the African forelands, 3=front of the Europe-verging Paleogene nappes, 4=front of the Africa-verging Paleogene nappes.

Subduction of continental lithosphere, as assumed by Alpine geologists (e.g. Laubscher, 1970), is not yet fully accepted by more orthodox supporters of plate tectonics. The problem of the buoyancy of the continental crust has been discussed by Molnar and Gray (1979), who smoothed some postulates arising from McKenzie's argumentations (1970). In conclusion, the dynamic aspect of the problem is far from being solved but some possible explanation may be found by assuming that during a continent-continent collision, the continental lid and the granulitic lower crust take part in the subduction, while the low-density upper crust is partly involved in nappe building and partly "nailed" in the roots of the chain.

#### ACKNOWLEDGEMENTS

The authors express their gratitude to C. Frohlich for access to his JHD computer program.

We are grateful to the staff of many seismological observatories, too numerous to list, for providing copies of seismograms.

#### REFERENCES

- Amodio Morelli, L., Bonardi, G., Colonna, V., Dietrich, D., Giunta, G., Ippolito, F., Liguori, V., Lorenzoni, S., Paglionico, A., Perrone, V., Piccarreta, G., Ruzzo, M., Scandone, P., Zanettin Lorenzoni, E. and Zupetta, A., 1976. L'arco calabro-peloritano nell'orogene appenninico-maghrebide. *Boll. Soc. Geol. Ital.*, 17: 1-60.
- Barberi, F., Bizouard, H., Capaldi, G., Ferrara, G., Gasparini, P., Innocenti, F., Jorono, J.L., Lambert, B., Treuil, M. and Allegre, C., 1977. Age and nature of basalts from the Tyrrhenian abyssal plane. Initial Rep., DSDP Leg 42A, Site 373A.
- Boccaletti, M. and Guazzone, C., 1972. Gli archi appenninici, il Mar Ligure ed il Tirreno nel quadro della tettonica dei bacini marginali retroarco. *Mem. Soc. Geol. Ital.*, 11: 21.
- Calcagnile, G., Fabbri, A., Farsi, F., Gallignani, P., Gasparini, C., Iannaccone, G., Mantovani, E., Panza, G.F., Sartori, R., Scandone, P. and Scarpa, R., 1981. Structure and evolution of the Tyrrhenian Basin. In: *Proceedings of the Commission Internationale pour l'Exploration Scientifique de la mer Méditerranée*. Cagliari, 27: 197-208.
- Cagnetti, V., Pasquale, V. and Polinari, S., 1978. Fault-plane solutions and stress regime in Italy and adjacent regions. *Tectonophysics*, 46: 239-250.
- Caputo, M. and Postpischl, D., 1973. Seismicity of the Italian region. *Quad. Ric. Sci.*, 90: 237-248.
- Caputo, M., Panza, G.F. and Postpischl, D., 1972. New evidences about deep structure of the Lipari arc. *Tectonophysics*, 15: 219-231.
- Cardwell, R.K. and Isacks, B.L., 1976. Investigation of the 1966 earthquake series in Northern China using the method of joint epicenter determination. *Seismol. Soc. Am. Bull.*, 66: 1965-1982.
- Del Pezzo, E., Luongo, G. and Scarpa, R., 1979. Seismic wave transmission in southern Tyrrhenian Sea. *Boll. Geofis. Teor. Appl.*, 21: 53-65.
- De Vivo, B., Dietrich, D., Guerra, I., Iannaccone, G., Luongo, G., Scandone, P., Scarpa, R. and Turco, E., 1979. Carta sismotettonica preliminare dello Appennino Meridionale. C.N.R.—Progetto Finalizzato Geodinamica, Pubbl., 166.
- Dewey, J.W., 1972. Seismicity and tectonics of Western Venezuela. *Bull. Seismol. Soc. Am.*, 62: 1711-1751.
- Douglas, A., 1967. Joint epicenter determination. *Nature*, 215: 47-48.
- Frohlich, C., 1979. An efficient method for joint hypocenter determination for large groups of earthquakes. *Comput. Geosci.*, 5: 387-389.
- Ghisetti, F. and Vezzani, L., 1979. Strutture crostali della Calabria e della Sicilia: loro evoluzione geodinamica. In: *Contributi preliminari alla sorveglianza e rischio vulcanico*. C.N.R.—Progetto Finalizzato Geodinamica, Pubbl., 235.
- Gutenberg, B. and Richter, C.F., 1948. Deep focus earthquakes in the Mediterranean region. *Geofis. Pura Appl.*, 12: 130-133.
- Herrin, E. (Editor), Arnold, E.P., Bolt, B.A., Clawson, G.E., Engdahl, E.R., Freedman, H.W., Gordon, D.W., Hales, A.L., Lobbell, J.L., Nuttli, O., Romney, C., Taggart, J. and Tucker, W., 1968. *Seismological tables for P phases*. *Seismol. Soc. Am. Bull.*, 58: 1193-1352.
- Kárník, V., 1969. *Seismicity of the European Area*. Reidel Publ. Co., Dordrecht.
- Knopoff, L., 1961. Analytical calculation of the fault-plane problem. *Publ. Dom. Obs.*, Ottawa, 24: 309-315.
- Laubscher, H.P., 1970. *Bewegung und Wärme in der Alpine Orogenese*. Schweiz Mineral. Petrogr. Mitt., 50: 565-596.

- Le Pichon, X., Francheteau, J. and Bonnin, J., 1973. *Plate Tectonics*. Elsevier, Amsterdam, 300 pp.
- McKenzie, D.D., 1970. Speculations on the consequences and causes of plate motion. *Geophys. J., R. Astron. Soc.*, 18: 1-18.
- McKenzie, D.D., 1972. Active tectonics of the Mediterranean region. *Geophys. J., R. Astron. Soc.*, 30: 109-185.
- Mechler, P. and Mseddi, R., 1977. Structure du manteau superieur sous la mer Mediterranée. *Publ. Inst. Geophys., Pol. Acad. Sci., A-4 (115)*: 331-346.
- Molnar, P. and Gray, D., 1979. Subduction of continental lithosphere: some constraints and uncertainties. *Geology*, 7: 58-62.
- Panza, G.F., 1979. The crust and upper mantle in Southern Italy from geophysical data. *Riv. Ital. Geofis.*, 5: 17-22.
- Qamar, A., 1974. Seismicity of the Baffin Bay region. *Bull. Seismol. Soc. Am.*, 64: 87-88.
- Richter, I. and Strobach, K., 1978. Benioff zones of the Aegean Arc. In: H. Closs, D. Roeder and K. Schmidt (Editors), *Alps, Apennines, Hellenides*. I.U.G.G. Sci. Rep., 38: 410-414.
- Ritsema, A.R., 1972. Deep earthquakes of the Tyrrhenian sea. *Geol. Mijnbouw*, 58: 541-545.
- Ritsema, A.R., 1979. Active or passive subduction at the Calabrian arc. *Geol. Mijnbouw*, 58(2): 127-134.
- Riuscetti, M. and Schick, R., 1975. Earthquakes and tectonics in Southern Italy. *Boll. Geofis. Teor. Appl.*, 17: 59-78.
- Rothé, J.P., 1969. The seismicity of the earth 1953-1965. UNESCO, Paris, *Earth Sci.*, 1.
- Scandone, P., 1979. Origin of the Tyrrhenian sea and Calabrian arc. *Boll. Soc. Geol. Ital.*, 98: 27-34.
- Scandone, P., Giunta, G. and Liguori, V., 1974. The connection between the Apulia and Sahara continental margins in the Southern Apennines and in Sicily. *Rapp. P-V. Reun., Cons. Int. Explor. Mer.*, 26e Congr., 23 (4A): 99-103.
- Scarpa, R., 1982. Travel-time residuals and three-dimensional velocity structure of Italy. In prep.
- Strobach, K., 1973. Curvature of island arcs and plate tectonics. *Z. Geophys.*, 39: 819-831.
- Wickens, A.J. and Hodgson, J.H., 1967. Computer re-evaluation of earthquake mechanism solutions. *Publ. Dom. Obs., Ottawa*, 33: 1-55.